Particle source and edge transport studies in JET H-mode gas puff modulation experiments

A. Salmi[1], T. Tala[1], P. Mantica[2], A. Järvinen[3], L. Meneses[4], S. Mordijck[5], V. Naulin[6], J. Juul Rasmussen[6], J. Svensson[7], L. Giacomelli[2], R. Gomes[4], M. Groth[3], T. Koskela[3], C. Maggi[8], M. Maslov[8], G. Sips[9], H. Weisen[10] and JET contributors*

EUROfusion Consortium, JET, Culham Science Centre, Abingdon, OX14 3DB, UK
[1]VTT, Espoo, Finland; [2]IFP, CNR-ENEA, Milan, Italy; [3]Aalto University, Helsinki, Finland; [4]IPFN, IST, Universidade de Lisboa, Portugal; [5]College of William & Mary, Virginia, USA; [6]DTU Physics, Lyngby, Denmark; [7]IPP, Greifswald, Germany; [8]CCFE, Abingdon, UK; [9]EFDA CSU, Culham, UK; [10]CRPP, Lausanne, Switzerland.

Gas modulation experiments in H-mode plasmas featuring a scan in collisionality to study particle transport and sources at the plasma edge have been carried out on JET [1,2]. The local electron density response to the gas injection was measured with reflectometer and Thompson scattering diagnostics close to the midplane. Modulation amplitudes below 1% (in the core) are reliably measured thus allowing minimal plasma disturbance and the possibility to use data from multiple harmonics. The linearity of the electron density response was verified in identical plasmas by having different gas modulation amplitudes.

The set of experiments were run in a corner configuration with strike points near the pumping ducts and gas modulation from top of the machine approximately from a point source. Figure 1 illustrates the plasma shape and density modulation due to the gas injection for the shot #87420 (B_T=2.67T, I_P=2MA). The propagation of the perturbation is clearly seen in the reflectometer signal up to mid radius yielding data for up to three harmonics.

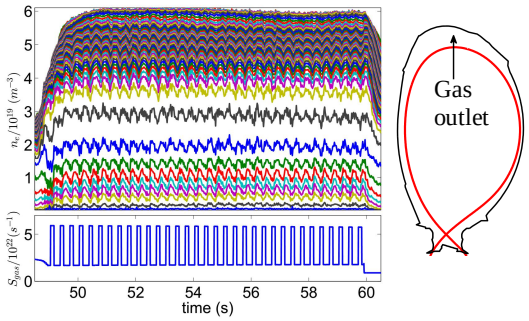

Figure 1 Experimental gas waveform and resulting density modulation. Top location (GIM7) was used for gas injection #87420.

Time resolved electron density measurements together with 1.5D transport modelling are used to clarify the mechanisms responsible for fuelling of the plasma. In particular we aim to understand whether plasma fuelling is due to inward convection or whether even in H-mode there could be significant source penetrating pedestal top. We assume that electron density obeys the following 1.5D equation with geometrical shape corrections included

$$\frac{\partial n_e}{\partial t} = \frac{1}{V'}\frac{\partial}{\partial \rho}\left[V'\left(\langle(\nabla\rho)^2\rangle D\frac{\partial n_e}{\partial \rho} - \langle\nabla\rho\rangle v n_e\right)\right] + S(\rho,t)$$

where ρ is the radial coordinate (=square root of normalised poloidal flux), $\langle\ \rangle$ denotes flux surface average, S is the particle source (including both cold neutrals and neutral beam (NB) ions) and V′ is the radial derivate of the plasma volume. We assume time independent radial profiles for the diffusion D and convection v. Here, the electron density profile n_e is measured as a function of time and the geometrical factors $\langle(\nabla\rho)^2\rangle$, $\langle\nabla\rho\rangle$ and V' are obtainded from EFIT equilibrium solver. The unknown $\boldsymbol{D}, \boldsymbol{v}$ and $\boldsymbol{S}$ are solved using an iterative scheme where they are varied inside a non-linear optimisation routine until the simulated electron density best matches the experimental data.

The 3 Hz rectangular gas modulation with ~35% duty cycle yields density perturbation above the noise level for up to 3rd harmonic. Experimental data thus provides us one real valued equation from the steady state and three complex valued equations from the three harmonics totalling to seven equations (we effectively use only 5 equations). As we have only three unknown profiles we have more than sufficient information to solve the unknowns simultaneously. The steady state equation provides us a relation between D, v and S thus eliminating one unknown:

$$v = \frac{\langle(\nabla\rho)^2\rangle}{\langle\nabla\rho\rangle}\frac{\frac{\partial\bar{n}_e}{\partial\rho}}{\bar{n}_e}D + \frac{\int_0^\rho V'\bar{S}d\rho}{\bar{n}_e V'\langle\nabla\rho\rangle}$$

We use the following parametrisation for D and S

$$D(\rho) = \frac{1}{2}(a_1 + a_2\rho^{a_3})\left(1 - \tanh\frac{\rho - a_4}{a_5}\right) + a_6$$

$$S(\rho, t) = S_{NBI} + a_7 \exp\left(\frac{1-\rho}{a_8}\right)\left(1 + a_9 S_t(t - a_{10})\right)$$

where the ten scalar coefficients a_x are optimised. The experimental gas waveform $S_t(t)$ is normalised such that $\bar{S}_t = 1$ and $\Delta S_t = 1$.The neutral beam particle source S_{NBI} is calculated with PENCIL. Figure 2 gives a graphical illustration of the free parameters.

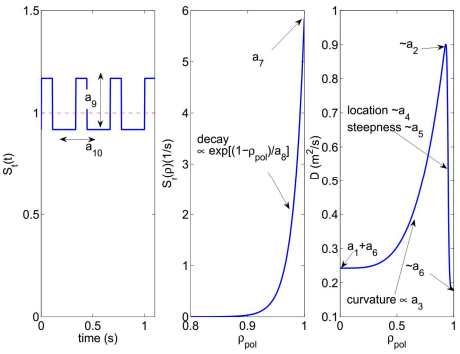

Figure 2 Parametrisation for D and S.

Figure 3 gives the result of the fitting when all parameters are allowed to be optimised (full black line) and when the source decay length (i.e. a_8) forced to be $8\ cm$ (dashed black line). We use reflectometer data for the three harmonic amplitudes and Thompson scattering diagnostic for the first harmonic phase profile. This is because at the moment we are still in the process of validating the phase profiles from processed reflectometer data. With this data set we are able to obtain a fit that reproduces the experimental data within the error bars ($\chi^2/N \sim 1$) thus improving on previous analysis [2]. Note that the experimental error bars include only statistical error of the data mapped on a fixed a coordinate system but not those that might arise due to mapping itself, other data processing or from other unknown sources. The small diffusion inside $\rho_{pol} < 0.6$ radius is essentially due to the rapidly decaying perturbation amplitude which is not reproduced with $D \sim 1\ m^2/s$. The resulting small diffusive flux Γ_D is then mostly balanced by the NB particle flux thus eliminating the need for inward convection to explain the peaked density profile. For more details please see [1].

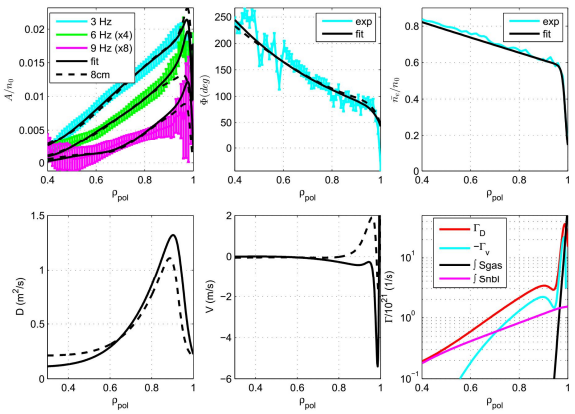

Figure 3 Experimental data compared against simulations on top row (amplitude, phase and average density) and the corresponsing diffusion and convection profiles together with the associated fluxes on the bottom row. Full black line is for narrow source (1cm) and dashed line for deep source (8cm).

The best overall fit is found with a relatively narrow cold neutral ionisation profile ($a_8 \sim 1\ cm$) which in turn requires inward convection at the edge. However, ionisation source widths of up to $8\ cm$ are equally well fitted inside $\rho_{pol} < 0.9$ while outside they start to deviate. Interestingly, when source width is fixed to a value larger than $\sim 2\ cm$ the additional source going across the pedestal cannot be compensated by increasing diffusion but outward convection is required as shown in dashed line for the $8\ cm$ case in Figure 3. As outward convection appears less likely than edge localised inward convection this could

indicate that the cold neutral ionisation source is not significantly penetrating the pedestal. Further gas modulation experiments in plasmas with more opaque SOL could potentially clarify this question. Regardless of the cold neutral source width it is the NB flux that contributes mostly to the density peaking in the core plasma. With the narrow source we found that the modulated incoming flux crossing the separatrix needed to fit the experiment is about 20% of the injected modulated gas and that the steady state flux is about twice the amount of the total gas fuelling. Typically these numbers have factor of 2 uncertainties.

In addition to core diagnostics the neutral sources were diagnosed with visible light divertor and wide angle cameras behind D_α and D_β filters. They were operated at maximum available framerate ($60\,Hz$) for the full duration of the discharge. Figure 4 shows the wide angle view of the D_β radiation. The bright spot at the top of the vessel is the gas injection location. One can observe that it is not only the actual injection point that features oscillations but that significant $3\,Hz$ component is present everywhere and especially at the divertor indicating that fuelling indeed modulates the recycling quite strongly. Furthermore, frame b) provides new insight on the time scales. The radiation peak and thus potentially also the maximum ionisation rate at the divertor takes place roughly $50\,ms$ after it appears at the top of the vessel. The time trace e), the spectrum f) and the error indicator d) illustrate periodicity and noise in the data. For long modulations, like in here, the time scales can possibly be estimated to less than $5\,ms$ accuracy.

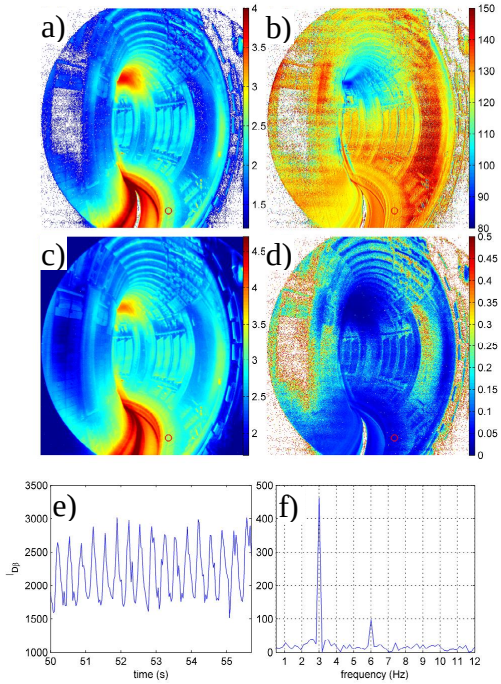

Figure 4 Wide angle camera D_β radiation. a) 3Hz amplitude, b) 3Hz phase, c) steady state, d) error indication $\delta A/A$, e) intensity at the red circle and f) spectrum at red circle.

Figure 5 shows the tomographic inversion [3,4] of the divertor camera D_α image on a 2D plane. Also here amplitude and average intensity are plotted on log scale. While the recycling is highest at the targets one can also see a 'plume' on the inner divertor apron clearly synchronised with the gas modulation that cycles the upstream conditions. It also appears that the recycling at this location is generating some higher energy neutrals that are able to penetrate deeper into the confined plasma. Furthermore, the frame b) shows that on the inside of the X-point the emission is decreasing when modulated gas is on which indicates that the inner strike point leg periodically detaches creating very cold and dense plasma during the added gas. Moreover, it is seen that D_α radiation peaks on the outer divertor $10-20\,ms$ after it peaks on the inner divertor. With a connection length of the order of $50\,m$ this would correspond to a sound speed of a $0.1\,eV$ deuteron which shows that parallel flow only cannot explain such a long difference. The coherent phase and the

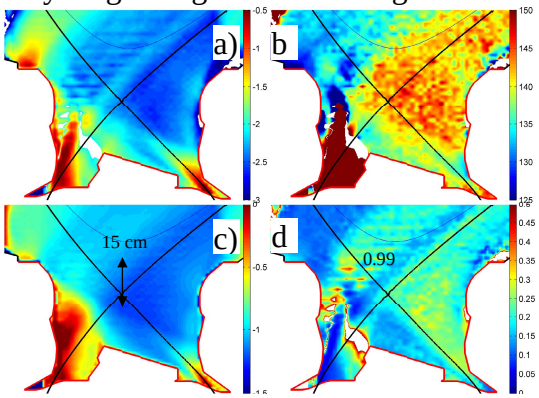

Figure 5 2D reconstruction [3,4] of divertor D_α camera with $\log_{10}$ colour scale. a) 3Hz amplitude, b) 3Hz phase, c) steady state, d) error $\delta A/A$. $\rho = 0.99$ surface is 1 cm from separatrix at midplane.

separatrix aligned amplitude together seem to suggest that cold neutrals are able to penetrate $10-15\ cm$ across the separatrix near the X-point, mainly on the LFS. However, as the plasma profiles steepen towards the midplane the penetration depth will also be reduced.

To better understand the recycling and ionisation profiles time dependent EDGE2D-EIRENE modelling was performed for roughly one modulation cycle. Figure 6 summarises the findings from this simulation. The underlying statistical noise and the lack of synthetic D_α and D_β diagnostics are obviously presenting challenges for comparisons against the camera data. Nevertheless, one can notice that modelling suggests that ionisation inside the separatrix is strongly concentrated on the low field side of the plasma (Figure 6a). However, these simulations do not include cross-field drifts or currents, and, therefore, the in-out divertor asymmetries are likely to be underestimated. As a result, the fractional contribution of LFS in the pedestal fuelling profile is probably overestimated relative to the HFS fuelling. The width of the flux surface averaged ionisation profile inside the separatrix is estimated to be roughly $1\ cm$ on the outboard mid plane being consistent with both the divertor camera and the 1.5D modelling. The dynamics of the simulated ionisation EDGE2D-EIRENE are rather complicated as seen on the phase plot (Figure 6b) and can vary significantly between neighbouring cells. Generally, they also seem quite fast compared to wide angle camera images. One possible contributing factor here could be that the actual source is essentially a point source but when communicated from EIRENE to EDGE2D it is made axisymmetric. Thus, 3D effects might need to be included to be able to reproduce the measured emissions and their relevant time scales.

To summarise: we have presented experimental data and modelling from gas modulation

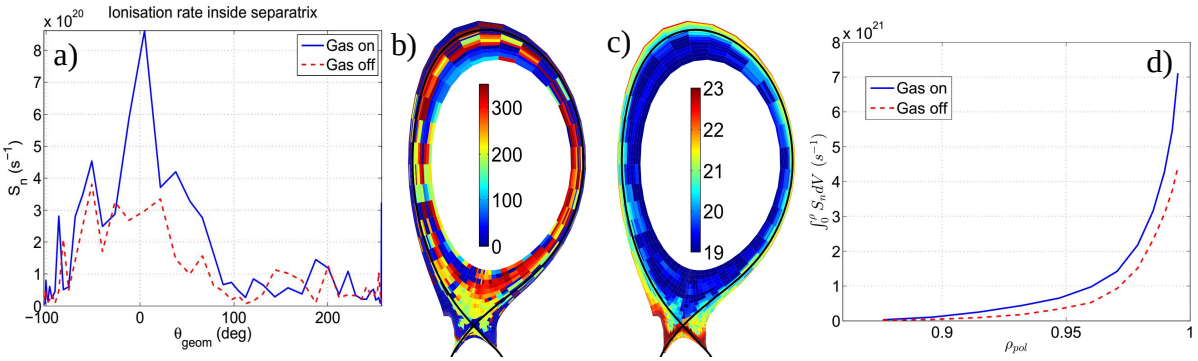

Figure 6 Ionisation rates and their 5 Hz phase and amplitude 2D profiles from EDGE2D-EIRENE simulations : a) ionisation rate inside separatrix, b) phase delay w.r.t. gas on time, c) $\log_{10}$ amplitude and d) radial ionisation profile

experiments that suggest that particle source inside separatrix is fairly narrow and it does not contribute much inside the pedestal top. Inward convection of the order of $5\ m/s$ at the plasma edge is needed to sustain the steep pedestal while the convection quickly drops to zero towards the core where small diffusion and NB source are responsible for the density peaking. But we also remind that as the error bars at the edge are large and potentially underestimated the wider source profiles cannot yet be ruled out with certainty.

[1] T. Tala et al. 2015 EPS, Portugal [2] A. Salmi et al. 2014 EPS, Germany
[3] J. Svensson 2011 EFDA–JET–PR(11)24 [4] J. Svensson et al 2007 Proc. IEEE WISP

** See the Appendix of F. Romanelli et al., Proc. 25th IAEA Fusion Energy Conference 2014, St Petersburg, Russia*